Critical-Field Study of Superconducting Aluminum*

SANDOR CAPLAN† AND GERALD CHANIN‡
University of Pittsburgh, Pittsburgh, Pennsylvania
(Received 4 January 1965)

The critical field of pure aluminum has been measured down to 0.28°K. Because the measurement technique requires a magnetic field gradient, both normal and superconductive phases were present in the sample, thus avoiding superheating and supercooling effects. The movement of the phase boundary in response to a change in magnetic field was continuously observed, its position at equilibrium leading to a determination of the critical field. Hysteresis in the transition was 0.3% of the critical field, with reduction to arbitrarily small values apparently possible. The deviation curve shows the usual weak-coupling characteristics and, apart from a low-temperature anomaly attributed to uncertainties in the vapor-pressure thermometry, good agreement with BCS theory. The measurements yield $T_c=1.175\pm0.001$°K and $(dH_c/dT)_{T_c}=158\pm4$ Oe/°K, while analysis of the low-temperature data indicates $H_0=104.8\pm0.6$ Oe with γ in the range 1.23 to 1.30 mJ/mole(°K)^2.

I. INTRODUCTION

DIRECT measurements of critical-field curves (H_c versus T) of "soft" superconductors are of interest primarily for their thermodynamic consequences. Magnetic measurements typically involve cylindrical samples in a longitudinal uniform field. Search coils about the sample are monitored by a ballistic galvanometer while the field is changed in small steps. The appearance of a signal during certain steps is taken as an indication of flux penetration at those field values, and therefore determines H_c. Reduction of the field in steps leads to the measurement of those steps during which flux is expelled. Ideally, for a long, thin, cylindrical, soft superconductor, these two field values should be equal to H_c, superheating and supercooling effects causing these fields to be different from each other and from the thermodynamic H_c. If departures from H_c result from some temperature-dependent physical mechanism,[1] the resultant systematic error in the critical-field curve may lead to very large errors in the thermodynamic quantities computed from its derivatives.

Table I shows the results of various experimental studies of aluminum. The large variations that remain after corrections for purity[1] and temperature scale[2,3] indicate that it would be useful to investigate the critical field of aluminum, being careful to minimize departures from thermodynamic equilibrium. In this experiment measurements were made on a sample containing both normal and superconducting phases, thus eliminating the possibility of superheating or supercooling effects. The position of the phase boundary could be continuously monitored over long time intervals, permitting a study of its movement to new equilibrium positions after changes in external fields.

II. EXPERIMENT

A. Samples

The single-crystal samples were grown by the Bridgman method from 99.999+% nominal-purity aluminum (Cominco Products, Spokane, Washington). To avoid contamination of the aluminum, the metal was melted in a high-vacuum furnace using a crucible made from high-purity graphite (AUC grade, National Carbon Company). The crucible could be separated into two halves in order to facilitate a strain-free removal of the cylindrical casting. As a precaution against contamination, the crucible was chemically cleaned after machining, then baked at 900°C in high

TABLE I. Results of previous studies of the critical-field parameters of aluminum.

Measurement method	T_c(°K)[a]	H_0(Oe)
Magnetic[b]	1.199	106
Magnetic[c]	1.173	96
Microwave absorption[d]	1.176	
Magnetic[e]	1.200	99
Calorimetric[f]	1.165	103
Microwave absorption[g]	1.176	
Thermal conductivity[h]	1.181	
Magnetic[i]	1.183	
Acoustic attenuation[j]	1.164	

[a] Temperature corrected for sample purity (see footnote 1) and for discrepancies between the temperature scale used and either the T_{58} He^4 vapor-pressure scale (see footnote 2) or the T_{62} He^3 vapor-pressure scale (see footnote 3).
[b] B. B. Goodman and E. B. Mendoza, Phil. Mag. **42**, 594 (1951).
[c] T. E. Faber, Proc. Roy. Soc. (London) **A231**, 353 (1955).
[d] M. A. Biondi, M. P. Garfunkel, and A. O. McCoubrey, Phys. Rev. **108**, 495 (1957).
[e] J. F. Cochran and D. E. Mapother, Phys. Rev. **111**, 132 (1958).
[f] N. E. Phillips, Phys. Rev. **114**, 676 (1959).
[g] M. A. Biondi and M. P. Garfunkel, Phys. Rev. **116**, 853 (1959).
[h] C. B. Satterthwaite, Phys. Rev. **125**, 873 (1962).
[i] D. C. Hopkins and D. E. Mapother, Bull. Am. Phys. Soc. **7**, 175 (1962).
[j] R. David, H. R. Van der Laan, and N. J.Poulis, Physica **29**, 357 (1963).

* This work was supported by the National Science Foundation and is based on the thesis of one of the authors (S. Caplan) submitted in partial fulfillment of the requirements for the M.S. degree.
† Present address: RCA Laboratories, Princeton, New Jersey.
‡ Present address: Service d'Aeronomie (C.N.R.S.), Verrieres-le-Buisson (Seine et Oise) France, and Institut d'Electronique, Faculte des Sciences, Orsay (Seine et Oise) France.
[1] G. Chanin, E. A. Lynton, and B. Serin, Phys. Rev. **114**, 719 (1959).
[2] F. G. Brickwedde, H. Van Dijk, M. Durieux, J. R. Clement, and J. K. Logan, J. Res. Natl. Bur. Std. **64A**, 1 (1960).
[3] R. H. Sherman, T. R. Roberts, and S. G. Sydoriak, Report No. LAMS-2701 (Office of Technical Services, Department of Commerce, Washington, D. C., Los Alamos, 1962).

vacuum (10^{-6} mm Hg). The first casting made with this crucible was discarded, the operation serving to leach out any remaining aluminum-soluble constituents.

After placing the aluminum-filled crucible in the vacuum furnace, the temperature was gradually increased to 700°C, the rate of increase being sufficiently slow to maintain the system pressure at or below 10^{-6} mm. After two hours at this temperature (40°C above the melting point), an atmosphere of He gas was admitted to insure that the melt conformed to the internal shape of the crucible. The high vacuum was restored after several minutes. Using a sliding vacuum seal, the crucible was slowly (about 1 in./h) withdrawn from the furnace, progressive solidification of the melt promoting the growth of a single crystal. After cooling to room temperature, the crucible was removed from the vacuum system and separated into its two halves at liquid-N_2 temperature, allowing the casting to slip free of the crucible without straining. A chemical etch confirmed its single-crystal character. The sample was annealed in the vacuum furnace at 600°C for 10 h, then gradually cooled to room temperature. Two single-crystal, cylindrical samples were made in this way, each of diameter 0.060 in. and about $5\frac{1}{2}$ in. long.

The high purity and freedom from imperfection of the finished samples may be inferred from the ratio of room-temperature resistance to that at 4.2°K. Samples of a different geometry (dish-shape) but prepared under similar conditions from the same ingot yielded $R_{300}/R_{4.2}$ values from 1800 to 2600.[4]

B. Apparatus

A conventional liquid He^4-liquid N_2 Dewar system contained the He^3 cryostat. The He^3 was protected against loss and contamination during its use and storage. Temperatures down to 0.28°K could be reached with an oil diffusion pump. Nonmagnetic and nonsuperconducting materials were used in the construction of the low-temperature portions of the cryostat and sample holder.

Within its vacuum jacket, the cryostat consisted of a copper He^3-bath container and a copper "sample block," thermally and mechanically linked by three brass tubes. The temperature of the "sample block"was regulated to within one millidegree during a one-hour measurement interval. Thermal gradients were avoided by mounting the temperature sensor (a 1200-Ω Speer carbon resistor) in the "sample block" while the heater was wound directly upon the bath container, the heat current travelling along the brass tubes. Power to the heater was electronically controlled from the unbalance of a Wheatstone bridge, of which the sensing resistor formed one arm. A He^3 vapor-pressure bulb in the "sample block" was the thermometer. Its pressure was measured with a high-precision McLeod gauge and the reading corrected for thermomolecular effects.[5] The temperature was determined using the T_{62} He^3 scale.[3]

The sample was mounted in a thin-walled, hollow cylinder holder. To avoid stresses, it was anchored only at one end by a bit of GE-7031 varnish. A set of pickup coils and a magnetic-field modulation coil were wound directly on the sample holder, coaxial with the sample. The total power dissipated in these coils was always well below 10^{-8} W. The sample holder was screwed tightly into place within the sample block, using silicon grease to improve the thermal contact.

A liquid-nitrogen-cooled solenoid with overwound ends provided a steady magnetic field parallel to the sample axis. Proton resonance was used to calibrate the field and to measure its gradient along the solenoid axis. The gradient was found to be 0.04% of applied field per centimeter in the region occupied by the sample. The earth's field in this region was nulled to less than 0.01 Oe by three pairs of Helmholtz coils surrounding the liquid N_2 Dewar. The solenoid current supply was observed to be stable to one part in 10^5 during intervals of one hour.

The magnetic-field modulation coil was driven at 10 cps, producing an ac field parallel to the sample. Its magnitude was always less than 0.01 Oe and was reduced to lower values near the transition temperature, so that the modulation field remained a small fraction of the critical field. A signal 90° out of phase with the modulation field was used as the reference voltage of a phase-sensitive detector.

The two pickup coils (each consisting of 5000 turns of No. 50 A.W.G. copper magnet wire wound directly on the sample holder, with a gap of $\frac{1}{4}$ in. between them) were connected in series opposition. The signal was amplified by a Nuvistor triode preamplifier[6] using an impedance-matching input transformer, and a Tektronix type-122 preamplifier. The signal component synchronous with the modulation field was obtained by the phase-sensitive detector and continuously displayed on a strip-chart recorder.

C. Measurements

In all measurements the sample started out in the superconducting state at zero field. The modulation field was applied and after the temperature was stabilized at the desired value the magnetic field was slowly increased to just below the expected critical-field value. With the pickup-coil signal continuously recorded, the magnetic field was slowly swept by a motor drive on the solenoid current supply. Sweep rates were of the order of 0.02 Oe/min, but slower rates were sometimes used.

Because of the field gradient, one end of the sample should become normal (while the rest remains super-

[4] M. A. Biondi, M. P. Garfunkel, and W. A. Thompson, Phys. Rev. **136**, A1471 (1964).

[5] T. R. Roberts and S. G. Sydoriak, Phys. Rev. **102**, 304 (1956).

[6] P. C. Caringella and W. L. Eisenman, Rev. Sci. Instr. **33**, 654 (1962).

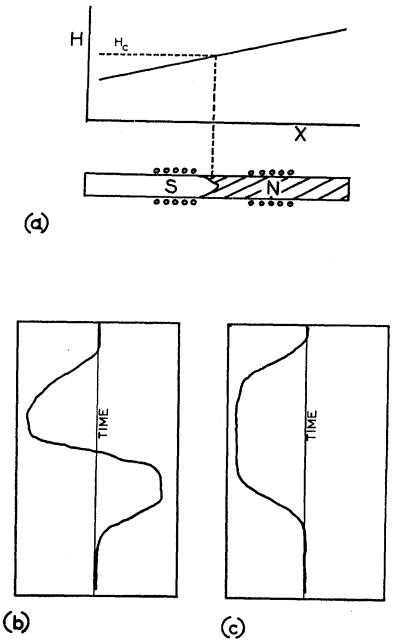

FIG. 1. (a) Production of a phase boundary by the magnetic-field gradient. Note position of pickup coils. (b) Recorder trace for a sweep through the critical field if the phase boundary were free to oscillate. (c) Recorder trace for a sweep through the critical field if the phase boundary were not free to oscillate.

conducting) as the local field increases, this normal region growing along the length of the sample and entering the region of the pickup coils [see Fig. 1(a)]. The boundary between the normal and superconducting phases should move back and forth along the sample in response to the 10-cps modulation field, in order to stay where the local field is H_c. As the boundary enters the first pickup coil, its output voltage will be of the order of $nAH_c(dx/dt)$, where n is the number of turns/cm of the coil, A is the cross-section area of the sample, and dx/dt is the velocity of the phase boundary. For a boundary completely free to follow the alternating field of the modulation coil, the motion is given by

$$dx/dt = (dH/dt)_{\text{mod}}/\text{grad}H_s,$$

where $(dH/dt)_{\text{mod}}$ refers to the modulation coil, and grad H_s is the field gradient of the liquid N_2 solenoid.

As described in II B, the quantity $\beta \equiv (\text{grad } H_s)/H_s = 4\times10^{-4}$ cm^{-1}. Since H_s is very nearly equal to H_c in order for a phase boundary to develop in the sample, the signal voltage is, to a good approximation, given by $(nA/\beta)(dH/dt)_{\text{mod}}$.

As the boundary moves into the second coil the same analysis would apply except for a change of sign. Thus with respect to the modulation field, the pickup-coil signal changes phase as the boundary moves from one coil to the next. The signal should therefore look like Fig. 1(b).

If the phase boundary could not oscillate in response to the modulation field only a variable mutual inductance effect would occur. The signal would be zero with the boundary absent from the coil region because of the opposed windings of the pickup coils. As the boundary penetrates the first coil the signal would increase, reaching a maximum when the boundary is between the two coils. As it passes through the second coil the signal would again decrease to zero. Note that there should be *no sign reversal* on the recorder chart, as shown in Fig. 1(c). The maximum signal voltage would be $nlA(dH/dt)_{\text{mod}}$, where l is the length of a coil, about 3 cm. The two mechanisms thus produce signal levels which differ by a factor of $1/(\beta l) \cong 10^3$, although this factor is somewhat exaggerated by the assumption that boundary motion is neither damped nor restricted. Because of this difference in signal level and because the experimental curves are like Fig. 1(b) rather than like Fig. 1(c), boundary oscillation appears to be the principle source of the signal.

During the course of the measurements, frequent readings of the He^3 vapor pressure and the solenoid current were noted on the recorder chart. This enabled a precise determination of that field at which the signal first crossed the zero level (corresponding to the boundary entering the region between the two coils). As the phase boundary would continue to drift even if the solenoid current were held stationary, the critical field was determined by stopping further increase of the solenoid current just after the initial rise of the curve. The chart recorder continues to trace out the curve, but at a much slower rate, eventually coming to rest at a

TABLE II. Critical-field measurements.

T (°K)	H_c (Oe)
0.278[a]	98.13
0.284[a]	97.96
0.287[b]	98.20
0.292[b]	97.78
0.300[b]	97.80
0.304[c]	97.23
0.308[c]	97.25
0.321[c]	96.54
0.323[c]	96.34
0.338	95.47
0.345	95.31
0.358	94.89
0.369	94.23
0.384	93.23
0.404	92.25
0.430	90.39
0.445	89.20
0.465	87.54
0.491	85.23
0.529	81.85
0.600	74.83
0.601	74.66
0.615	73.32
0.711	62.57
0.861	44.64
0.962	31.26
1.039	20.99
1.065	16.91
1.093	12.80
1.123	8.22
1.139	5.68
1.153	4.01
1.154	3.07
1.165	1.38
1.169	1.06

Uncertainties in absolute temperatures range from (see text):
[a] $\Delta T = \pm 0.020$°K.
[b] $\Delta T = \pm 0.015$°K.
[c] $\Delta T = \pm 0.010$°K.

value near the first zero crossing. ("Coming to rest" is a relative term limited by the stability of field and temperature, and here means no significant change for more than 10 min.) The field value at the point between the two pickup coils is then considered to be the critical field. If the field is now increased slightly (about 0.02%), the usual curve will be completed. If the field is reduced somewhat the curve will reverse itself, indicating the boundary is retreating. This usually required a field decrease of 0.3% (more at the higher temperatures) and indicates the upper limit of any possible hysteresis. It must be emphasized that our results indicate that the boundary responds to very small field changes and that the minimum field change necessary to make the boundary advance or retreat depends only on the amount of time allocated for the observation. However, if the field is increased well above the critical field so that the phase boundary disappears from the sample the usual supercooling effects are noticed upon subsequent reduction of the field.

D. Critical-Field Data

Although two samples were made, the data presented in Table II represent a single specimen. Measurements of the sample gave identical results for the critical-field values, but as the hysteresis under identical measuring conditions was slightly greater it was decided to restrict the experiment to the better sample. In the table, all temperatures are from the T_{62} He^3 scale[3] with appropriate thermomolecular corrections.[5] Data were taken in radom sequence. In spite of several warmups to liquid-nitrogen temperature, no changes in the critical field or in its hysteresis were observed.

III. ANALYSIS

A. Critical Temperature T_c and $(dH_c/dT)_{T_c}$

The critical temperature was determined graphically from linear fits of H_c versus T and H_c versus T^2. Both yield $T_c=1.175\pm0.001$°K.

The slope of the critical-field curve in the neighborhood of T_c was determined graphically. The result is

$$(dH_c/dT)_{T_c}=158\pm4 \text{ Oe/°K}.$$

B. Deviation Curve and Determination of H_0

A plot of critical field versus square of reduced temperature was extrapolated to yield an approximate H_0 of 104 to 105 Oe. The details of the critical field curve are best shown by plotting its deviation from a parabolic field. In Fig. 2 this deviation,

$$D\equiv H_c/H_0-[1-(T/T_c)^2]$$

(where H_0 is taken as 104.8 Oe), is plotted *versus* t^2. Below $t^2=0.1$, the large uncertainties and scatter arise primarily from the lack of reliable temperature data. McLeod gauge readings of the He^3 vapor pressure were in the range 5 to 20 μ Hg with considerable scatter at each temperature (about 3 μ) due to sticking of the mercury. A small bore ($\frac{1}{8}$-in.) measuring tube to the vapor pressure bulb necessitated large and temperature-sensitive thermomolecular corrections[5]; e.g., from a factor of 3 near $t^2=0.085$ to a factor of 6 near 0.057. The corresponding uncertainties in D range from $\Delta D=\pm0.003$ to $\Delta D=\pm0.010$. For this reason an extrapolation cannot yield precise results. The data appear to be consistent with an H_0 of 104.8 Oe (solid curve in Fig. 2). A choice of H_0 0.6 Oe higher or lower would be indicated if the data were fitted by the dashed or dot-dashed curves. (Renormalization to the new H_0 would, of course, make these curves also approach the origin.)

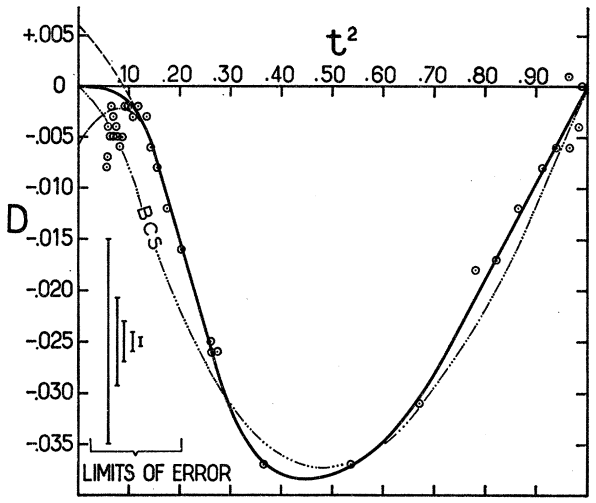

FIG. 2. Deviation from parabolic behavior D versus the square of reduced temperature: $D=H/H_0-[1-t^2]$, where $t=T/T_c$, $T_c=1.175$°K, and $H_0=104.8$ Oe. The theoretical curve labeled BCS is taken from Ref. 7. See text for discussion of sources of error below $t^2=0.10$.

The BCS theory of superconductivity predicts the curve[7] labeled BCS in Fig. 2. In contrast to the behavior of other weak-coupling superconductors such as S_n and T_a,[7] the data gives good agreement for the maximum deviation as well as for the general shape.

C. Entropy Difference ΔS

The entropy difference between the normal and superconductive states may be deduced from the curve in Fig. 2. Noting that[8]

$$\Delta S=S_N-S_S=-(V/8\pi)(d(H_c^2)/dT),$$

we obtain

$$\Delta S=\frac{VH_0^2}{2\pi T_c}ht\left[1-\frac{dD}{dt^2}\right],$$

or

$$\Delta S=\frac{VH_0^2}{2\pi T_c}ht\left[1-\frac{1}{2t}\frac{dD}{dt}\right].$$

[7] J. C. Swihart, IBM J. Res. Develop. 6, 14 (1962).
[8] D. Shoenberg, *Superconductivity* (Cambridge University Press, New York, 1952), Chap. III.

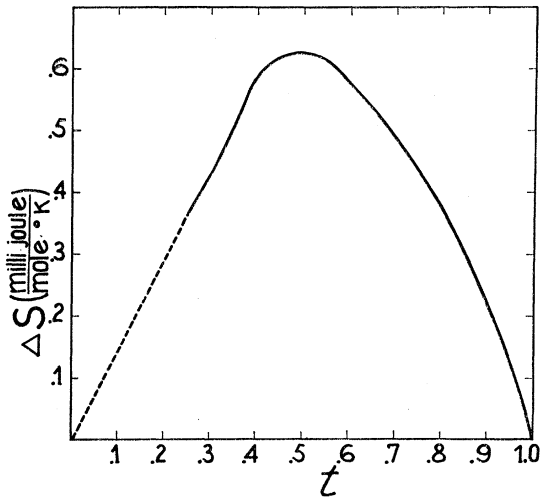

FIG. 3. Entropy difference between normal and superconductive states versus reduced temperature: $\Delta S = S_N - S_S$.

The slopes dD/dt and dD/dt^2 are obtained from the curve of Fig. 2 and from a plot of D versus t. The average ΔS obtained by these two methods is plotted versus reduced temperature in Fig. 3.

D. Normal State Heat Capacity

If we take the lattice heat capacity of the normal and superconductive states to be equal, and assume the superconductive-state electronic heat capacity is exponential,[9] we have for the difference of heat capacities:

$$\gamma T - a\gamma T_c e^{-bT_c/T} = T(d(\Delta S)/dT).$$

Integrating from 0 and T,

$$\gamma T - a\gamma T_c \int_0^T \frac{e^{-bT_c/T}}{T} dT = \Delta S.$$

Upon changing the variable of integration to $v = bT_c/T = b/T$, we have

$$\gamma T - a\gamma T_c \int_{b/t}^{\infty} \frac{e^{-v}}{v} dv = \Delta S.$$

The integral is the tabulated exponential function $-Ei(-b/t)$ so this equation may be written as[10]

$$\gamma T_c\{t - a[-Ei(-b/t)]\} = \Delta S.$$

For a given reduced temperature t, we may obtain ΔS as in Sec. C. Values of a and b may be taken as[11] $a = 7.1$, $b = 1.34$. The equation may then be solved for γ. The results are relatively insensitive to the choice of a and b at the lowest temperatures, becoming more sensitive at intermediate temperatures where the superconductive heat capacity becomes comparable to that of the normal state. At higher temperatures (above $t = 0.6$), where exponential dependence is no longer obeyed, the equation becomes invalid. Our results are given in Table III. Also given are the results for a different choice of parameters: $a = 9$, $b = 1.5$. Since the low-temperature results are the least sensitive to the choice of a and b, our results seem to indicate a value of γ between 1.23 and 1.30 mJ/mole (°K)^2, somewhat smaller than that measured by Phillips.[11]

TABLE III. Values of γ deduced from critical-field curve.

Reduced t	γ_1[a] mJ/mole (°K)^2	γ_2[a] mJ/mole (°K)^2
0.25	1.23	1.23
0.30	1.23	1.25
0.33	1.25	1.28
0.35	1.29	1.34
0.38	1.38	1.43
0.40	1.40	1.45
0.45	1.40	1.47
0.50	1.39	1.47
0.55	1.36	1.46

[a] The dependence upon the superconductive heat capacity, $C_S = \gamma a T_c e^{-b/t}$ is shown by calculating γ_1 for $a = 9$, $b = 1.5$ and γ_2 for $a = 7.1$, $b = 1.34$.

We may add that a second integration over temperature results in the following equation useful in analysis of critical field data because the field and temperature enter directly, without recourse to first or second derivatives:

$$H_c^2 = H_0^2 - (8\pi T_c^2 \gamma/V) \times\{(t^2/2) - a(b+t)[-Ei(-b/t)] - ate^{-b/t}\}.$$

IV. CONCLUSIONS

The critical-field curve of aluminum has been measured by a method which reduces hysteresis to 0.3% of the critical field. The residual hysteresis was inversely proportional to the time alloted for the observation of a change in equilibrium position of the phase boundary corresponding to the change in field. Qualitatively, the propagation velocity of the phase boundary was proportional to the difference between the local field and the critical field, and inversely proportional to temperature. This is in agreement with studies of the propagation of the phase boundary.[12,13]

It would seem that very precise critical-field studies could be made, the only apparent barriers to zero hysteresis being the long-term stability of temperature and magnetic field, and the patience and endurance of the investigator. However, the ability of the boundary to respond to a 10-cps modulation field while at the same time changing its position only very slowly in response to a change in the dc field raises some doubts about this technique. Perhaps the boundary surface is "pinned" at a discrete number of points of low surface energy, but the rest of it is relatively free to oscillate in syn-

[9] J. Bardeen, L. N. Cooper, and J. R. Schrieffer, Phys. Rev. **108**, 1175 (1957).
[10] E. A. Lynton, B. Serin, and M. Zucker, J. Phys. Chem. Solids **3**, 165 (1957).
[11] N. E. Phillips, Phys. Rev. **114**, 676 (1959).
[12] T. E. Faber, Proc. Roy. Soc. (London) **A223**, 174 (1954).
[13] T. E. Faber and A. B. Pippard, *Progress In Low Physics* (North-Holland Publishing Company, Amsterdam, 1957), Vol. 1, Chap. 9.

chronism with the modulation field. The long-distance mobility (its response to changes in the dc field) would then be limited by the nature and distribution of the "pinning" centers while the amplitude of oscillation would be limited by the bulk surface energy. Further investigations into these effects are in progress.

ACKNOWLEDGMENTS

The authors wish to thank Professor M. P. Garfunkel for his continued interest and encouragement. We are also very pleased to acknowledge the contributions of Joseph Pedulla for the solenoid calibration and for assisting with the data taking.

PHYSICAL REVIEW VOLUME 138, NUMBER 5A 31 MAY 1965

Variational Calculation for the Ising Model*

B. V. THOMPSON†
Carnegie Institute of Technology, Pittsburgh, Pennsylvania
(Received 11 January 1965)

The partition function of the Ising model with N spins, written as a functional integral, is approximated by replacing the field ψ_l at the lattice site l by the root-mean-square value of these fields, and evaluating the integral by a saddle-point method. A phase transition, whose mechanism is mathematically similar to that of the spherical model, is predicted at a temperature lower than the Weiss critical temperature. After parametrizing the mean-square field, one may apply a general variational principle to choose the parameters which minimize the difference between the approximate free energy and the exact Ising-model free energy. This optimum choice leads to the Horwitz-Callen theory.

I. INTRODUCTION

IT is well known that the partition function for the Ising model may be written in the form of a Gaussian average[1] or functional integral:

$$Z=\langle\prod_l Z_1(\psi_l)\rangle_G, \tag{1.1}$$

where Z_1 is the partition function for a single spin μ_l in an external field ψ_l:

$$Z_1(\psi_l)=\sum_{\mu_l=\pm1}\exp\mu_l\psi_l=2\cosh\psi_l.$$

The field ψ_l is a linear form in a set of random variables $\{x_\alpha\}$; and the average denoted by $\langle\ \rangle_G$ is taken over a Gaussian distribution of these variables

$$\langle F\rangle=\int\prod_\alpha\left(\frac{N}{\pi}\right)^{1/2}dx_\alpha[\exp-\sum_\alpha Nx_\alpha{}^2]F\{x_\alpha\}. \tag{1.2}$$

A review of the derivation of these formulas is given in Appendix A.

Consider the Ising lattice with an interaction energy

$$H=-\tfrac{1}{2}\sum_{ll'}V_{ll'}\mu_l\mu_{l'}.$$

We define the Fourier expansion

$$V_{ll'}=N^{-1}\sum_{\mathbf{k}}v_{\mathbf{k}}e^{i\mathbf{k}\cdot(\mathbf{l}-\mathbf{l}')},$$

where the $\mathbf{k}$'s are the set of N wave vectors appropriate to a translationally symmetric lattice with periodic boundary conditions. It is then convenient to let the x_α's be a set of $2N$ variables which we call $\{x_k,y_k\}$; and then (see Appendix A)

$$\psi_l=\sum_{\mathbf{k}}(2\beta v_{\mathbf{k}})^{1/2}(x_{\mathbf{k}}\cos\mathbf{k}\cdot\mathbf{l}+y_{\mathbf{k}}\sin\mathbf{k}\cdot\mathbf{l}). \tag{1.3}$$

The functional integral (1.1) has been approximated by a saddle-point method; that is, one writes

$$Z=\int\prod_\alpha\left(\frac{N}{\pi}\right)^{1/2}dx_\alpha e^{NY\{x_\alpha\}}, \tag{1.4}$$

where

$$Y\{x_\alpha\}=-\sum_{\mathbf{k}}(x_k{}^2+y_k{}^2)+N^{-1}\sum_l\ln2\cosh\psi_l. \tag{1.5}$$

One then assumes that the integral is dominated by a single peak in the integrand whose location is determined by

$$\partial Y/\partial x_\alpha=0\quad\text{at}\quad\{x\}=\{x_s\}.$$

The dominant peak in $Y\{x_k,y_k\}$ is easily seen to lie along the x_0 axis, where the stationary point x_{0s}, satisfies

$$(\partial Y/\partial x_0)\,|_s=x_{0s}-(2\beta v_0)^{1/2}\tanh(2\beta v_0)^{1/2}x_{0s}=0.$$

This is equivalent to the magnetization equation in the Weiss theory. For $\beta=(kT)^{-1}<\beta_c=v_0{}^{-1}$, x_{0s} is zero; whereas for $\beta>\beta_c$, x_{0s} is proportional to the nonvanishing spontaneous magnetization. The derived

* Supported in part by the National Science Foundation.
† Present address: Manchester College of Science and Technology, England.
[1] A. J. F. Siegert, *Brandeis Lectures* (W. A. Benjamin, Inc., New York, 1962), Vol. 3.